Electronic Supplementary Information (ESI)

A model study of ceria-Pt electrocatalysts: stability, redox properties and hydrogen intercalation

Lukáš Fusek,[1,2] Pankaj Kumar Samal,[1] Jiří Keresteš,[1] Ivan Khalakhan,[1] Viktor Johánek,[1] Yaroslava Lykhach,[2] Jörg Libuda,[2] Olaf Brummel,[2,*] and Josef Mysliveček[1,*]

[1]Charles University, Faculty of Mathematics and Physics, Department of Surface and Plasma Science, V Holešovičkách 2, 180 00 Praha 8, Czech Republic

[2]Interface Research and Catalysis, Friedrich-Alexander-Universität Erlangen-Nürnberg, Egerlandstr. 3, 91058 Erlangen, Germany.

[*]josef.myslivecek@mff.cuni.cz, olaf.brummel@fau.de

Figures S1-S9, Tables S1, S2, Materials and Methods, References

Data Availability:

Original experimental data are available via Zenodo, DOI: 10.5281/zenodo.8231965

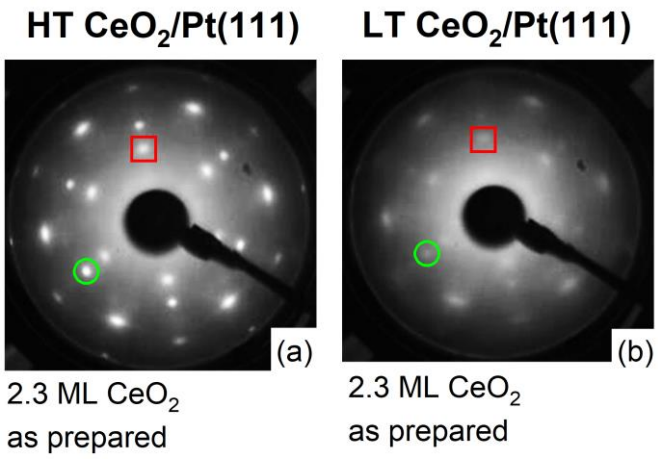

Figure S1: LEED diffraction patterns showing Pt(111) and CeO_2(111) spots for HT and LT samples. Pt(111) and CeO_2(111) are marked with a circle/a square, respectively.

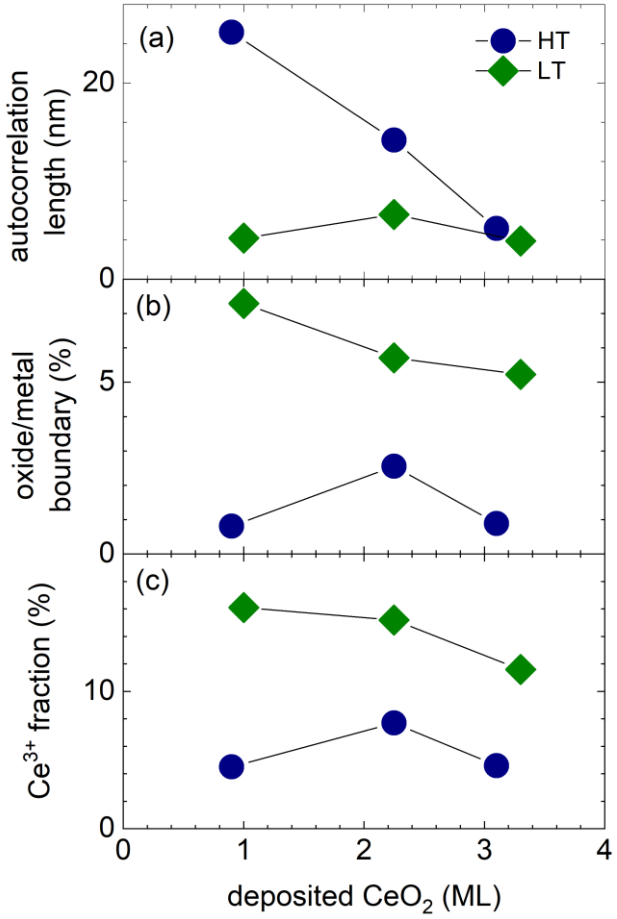

Figure S2: Comparison of chemical and morphological properties of the as-prepared HT and LT samples as a function of the amount of deposited CeO_2. (a) autocorrelation length of the samples. (b) extent of the oxide/metal boundary on the samples determined as a fraction of substrate Pt atoms localized at the oxide/metal boundary. (c) fraction of Ce^{3+} contribution in the Ce 3d XPS spectra of the samples. Lines represent guides to the eyes.

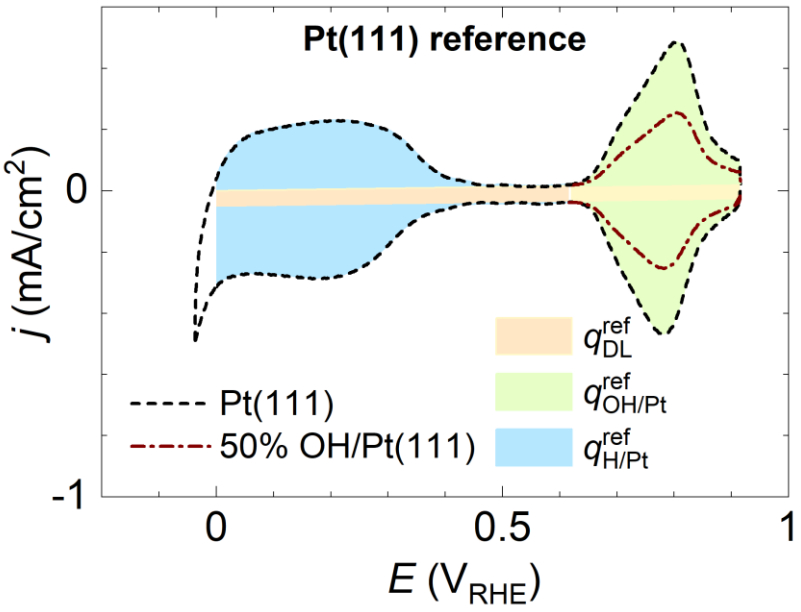

Figure S3: Reference experimental CV of a clean Pt(111) sample (0.1 M KOH, 400 mV/s). Color shading indicates a total integrated charge assigned to the double layer ($q^{ref}_{DL)}$, to H adsorption/desorption ($q^{ref}_{H/Pt}$), and to OH adsorption/desorption ($q^{ref}_{OH/Pt}$). q^{ref}_{DL} =125 μC/cm^2, $q^{ref}_{H/Pt}$= 350 μC/cm^2, and $q^{ref}_{OH/Pt}$ = 305 μC/cm^2 in good agreement with values reported in the literature.[1] All charges are integrated between 0 and 0.9 V_{RHE}. Scaling of the reference CV for clean Pt(111) for determining the Ce^{3+}/Ce^{4+} charge in CVs of ceria/Pt: charge in the OH adsorption/desorption region is reduced by a particular scaling factor (here 50%, dash-dotted curve). Charges in the H adsorption/desorption and the double layer charge remain unchanged.

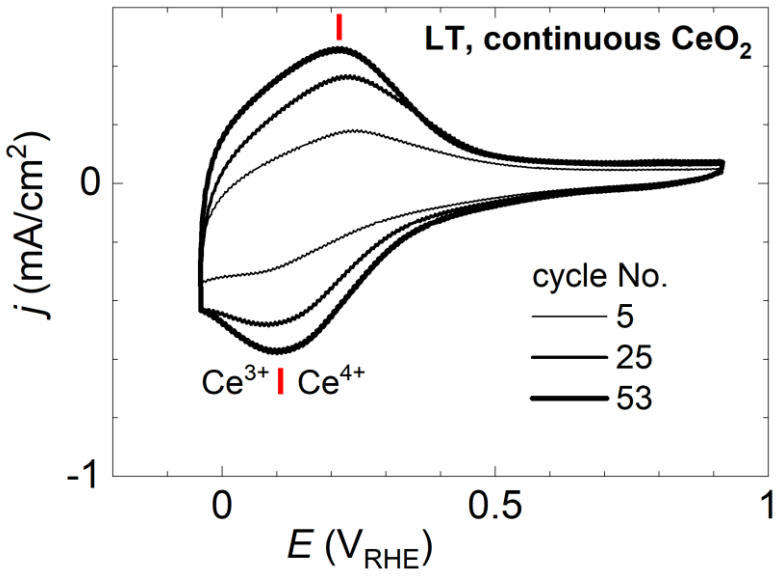

Figure S4: Cyclic voltammetry of a continuous CeO_2(111) thin film on Pt(111) (0.1 M KOH, 400 mV/s). Stability of the CV for subsequent cycles. Red ticks indicate the positions of Ce^{3+}/Ce^{4+} redox peaks.

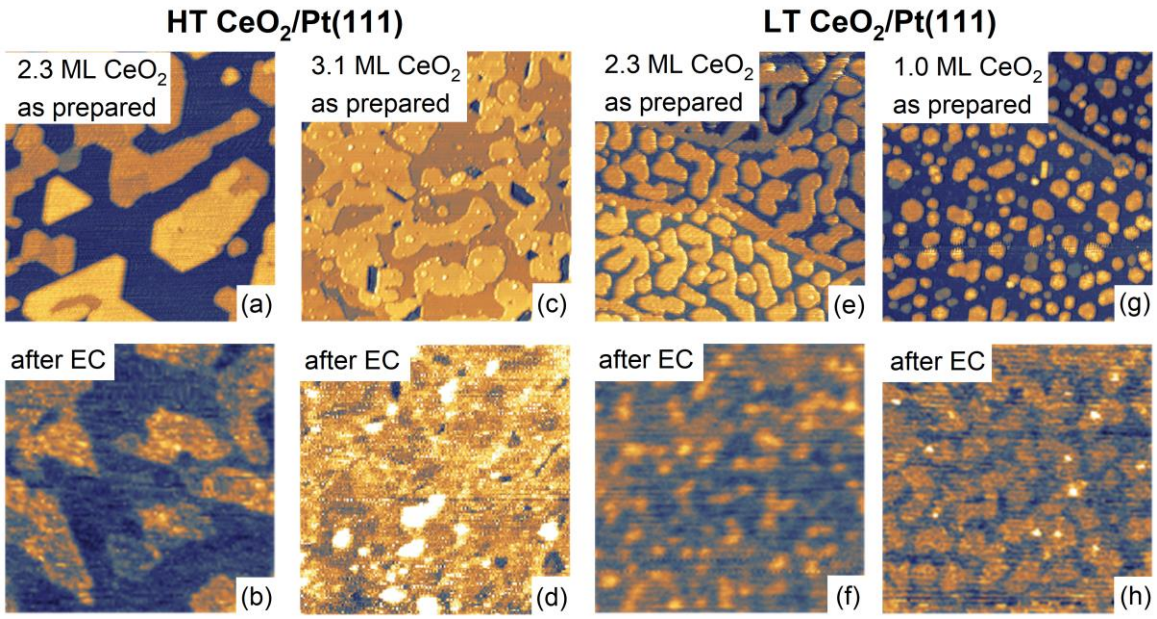

Figure S5: Comparison of morphology of the as-prepared samples (a, c, e, g - STM in UHV) and after EC characterization. (b, d, f, h – AFM in air). All images 150×150 nm^2.

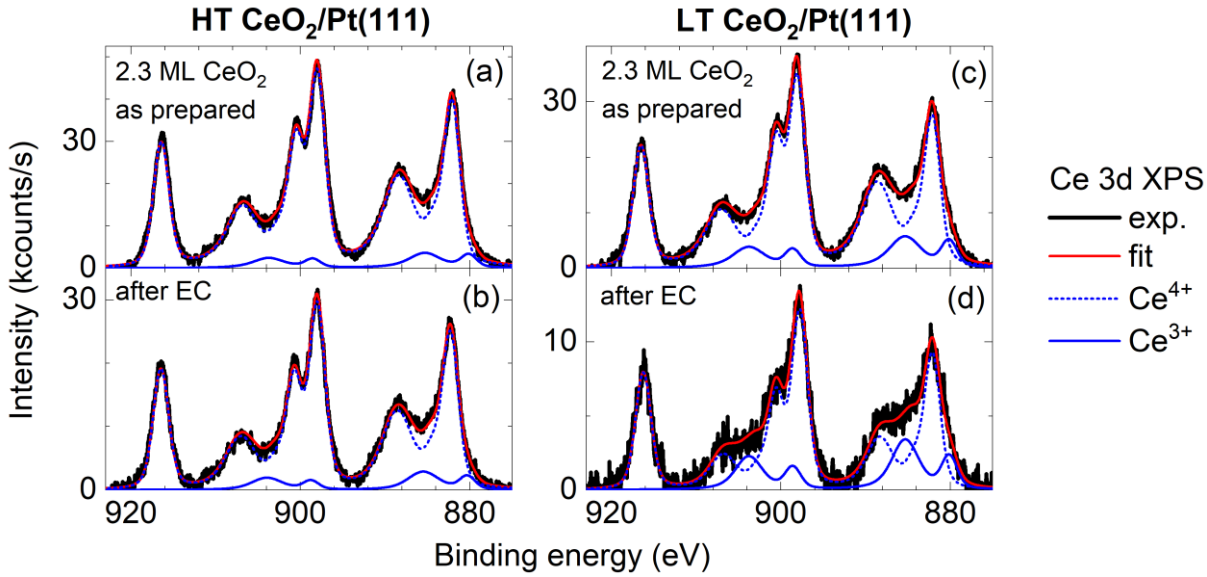

Figure S6: Comparison Ce 3d XPS spectra of the as-prepared samples (a, c) and after EC and AFM characterization in air (b, d). Ce^{3+} and Ce^{4+} contributions in the spectra are indicated by solid and dotted blue lines, respectively. Ce^{3+} fraction in Ce 3d XPS spectra is 8, 9, 15, and 23% in (a), (b), (c), and (d), respectively.

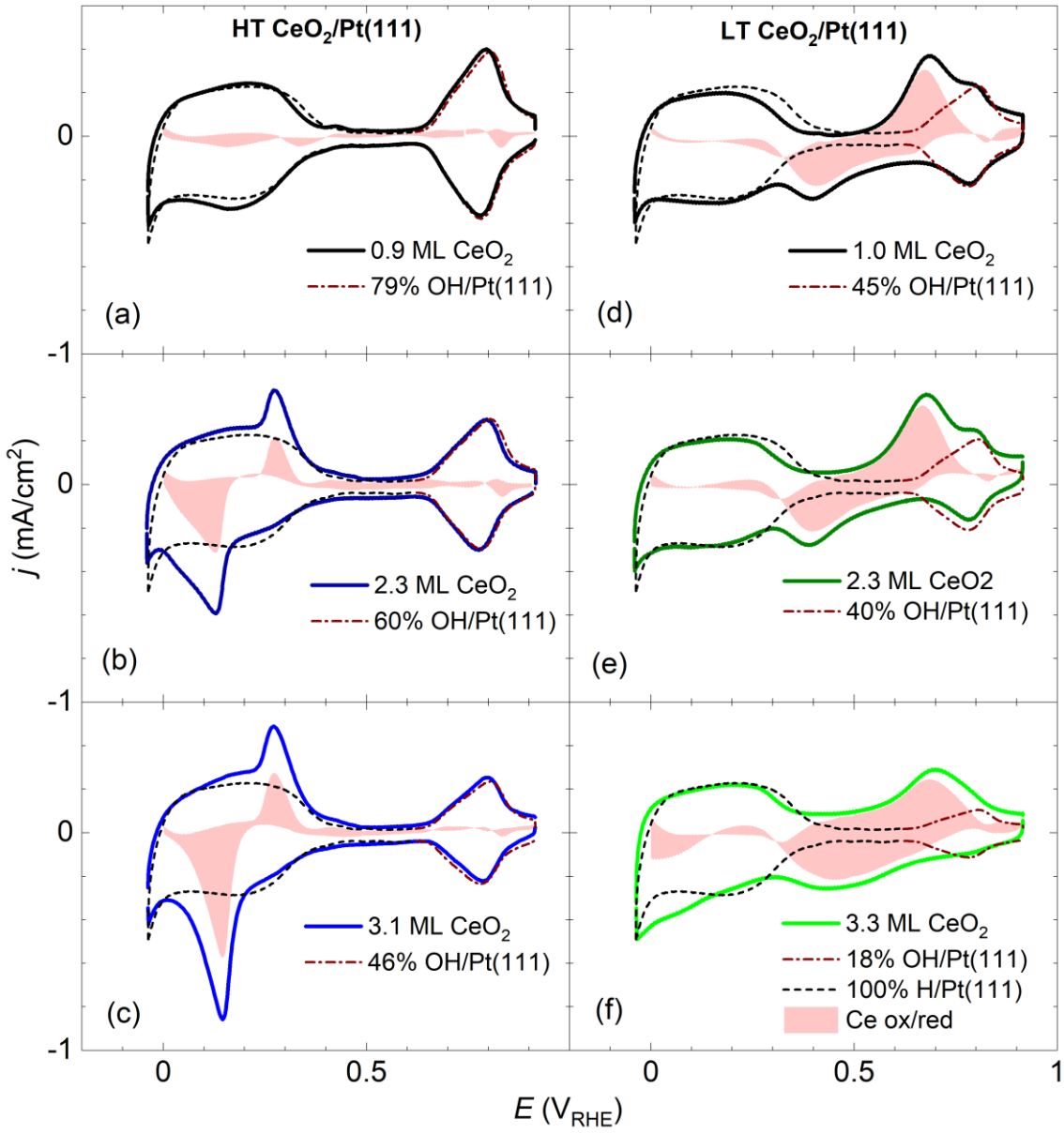

Figure S7: Determination of the Faradaic contribution to Ce^{3+}/Ce^{4+} electrooxidation/reduction for samples from Figures 1 and 2. Red shaded area represents a difference between the experimental CV of a ceria/Pt sample (solid line) and scaled reference data for clean Pt(111). The scaling factors of OH/Pt(111) regions represent the fraction of the electrochemically active clean Pt(111) area θ^{Pt}_{EC} on the corresponding ceria/Pt samples.

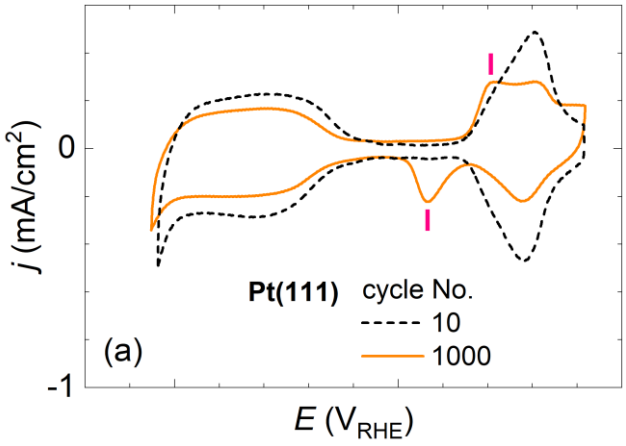

Figure S8: CVs of clean Pt(111), and Pt(111) upon prolonged cycling (1000 cycles, 0.1M KOH, 400 mV/s). Irreversible peaks marked by pink ticks are assigned to adventitious deposition of transition metal oxyhydroxides from the electrolyte solution.[2] Note that contrary to ceria nanoislands on Pt(111) surface (Figure 2), transition metal oxyhydroxide deposit blocks both the OH adsorption/desorption and H adsorption/desorption on Pt(111).

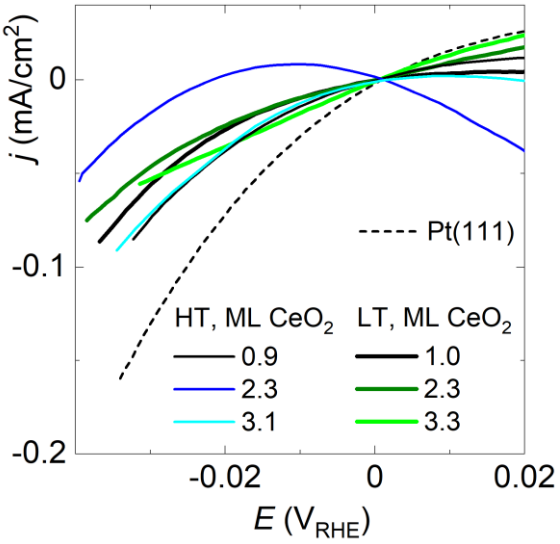

Figure S9: Comparative view of the onset of hydrogen evolution reaction in the CVs of HT and LT samples from Figures 1, 2.

Table S1

Parameters of the CeO_2/Pt(111) samples after preparation in UHV. Samples presented in the main text. Preparation method: HT – deposition of Ce metal in O_2 atmosphere at RT, subsequent annealing in O_2 atmosphere at 1050 K. LT – deposition of Ce metal in O_2 atmosphere at 523 K, subsequent annealing in O_2 atmosphere at 850 K. HT', LT' – two-step deposition and annealing. CeO_2 coverage upper estimate from STM images, lower estimate from CeO_2 deposited amount. CeO_2 average and max. thickness form STM images. Ce^{3+} fraction in per cent of total Ce 3d signal from XPS (cf. Figure S6). Length of CeO_2/Pt boundary in per cent of Pt(111) surface sites from STM images. Autocorrelation length from STM images. Reference clean Pt(111) was prepared, characterized, and results presented in Figures 2, 5, S3, and S7-S9.

sample No.	prep. method	CeO_2 amount (ML)	CeO_2 coverage upper estimate (%)	CeO_2 coverage lower estimate (%)	CeO_2 average thickness (ML)	CeO_2 max thickness (ML)	Ce^{3+} fraction (%)	CeO_2/Pt bound. (%)	auto-corr. length (nm)	Figure
1	HT	0.9±0.1	26	18	5.0±1.0	5	4.5±2.5	0.8±0.1	25±3	1 a, 2, 4, 5, S2, S5, S7, S9
2	HT	2.3±0.2	55	45	4.0±1.0	5	7.7±2.5	2.6±0.3	14±4	1 b, 2, 4, 5, S2, S5, S7, S9
3	HT	3.1±0.3	96	62	3.7±1.0	5	4.6±2.5	0.9±0.1	5±1	1 c, 2, 4, 5, S2, S5, S7, S9
4	HT'	3.8±0.4	22	n. a.	n. a.	n. a.	4.0±2.5	n. a.	22±3	3 a
5	LT	1.0±0.1	43	25	3.4±1.0	4	16±2.5	7.3±0.7	4±1	1 d, 2, 4, 5, S2, S5, S7, S9
6	LT	2.3±0.2	64	45	3.8±1.0	5	15±2.5	5.7±0.6	7±2	1 e, 2, 4, 5, S2, S5, S6 c, S6 d, S7, S9
7	LT'	3.3±0.3	82	66	4.3±1.0	5	12±2.5	5.2±0.5	4±1	1 f, 2, 3 b, 4, 5, S2, S5, S7, S9
8	Pt(111) clean	0	0	0	0	0	0	0	n. a.	2, 5, S3, S7-S9

Table S2

Parameters of the CeO_2/Pt(111) samples after preparation in UHV. Samples presented in the Supplementary information (ESI). Preparation method: HT – deposition of Ce metal in O_2 atmosphere at RT, subsequent annealing in O_2 atmosphere at 1050 K. LT – deposition of Ce metal in O_2 atmosphere at 523 K, subsequent annealing in O_2 atmosphere at 850 K. LT'' – deposition of Ce metal in O_2 atmosphere at 523 K, subsequent annealing in O_2 atmosphere at 523 K. CeO_2 coverage upper estimate from STM images, lower estimate from CeO_2 deposited amount. Ce^{3+} fraction in per cent of total Ce 3d signal from XPS (cf. Figure S6). Reference Pt(111) with nanoislands of transition metal oxyhydroxide was prepared by extended cycling in 0.1 M KOH (1000 cycles), characterized, and results presented in Figure S8.

sample No.	prep. method	CeO_2 amount (ML)	CeO_2 coverage upper estimate (%)	CeO_2 coverage lower estimate (%)	Ce^{3+} fraction (%)	CeO_2/ Pt bound. (%)	Figure
9	LT''	13.5±1	100	100	0±2.5	0	S4
10	HT	2.3±0.2	n. a.	n. a.	n. a.	n. a.	S1 a
11	LT	2.3±0.2	n. a.	n. a.	n. a.	n. a.	S1 b
12	HT	2.3±0.2	n. a.	n. a.	8±2.5	n. a.	S6 a, b
13	Pt(111) w. transition metal oxohydr.	0	0	0	0	0	S8

Materials and methods:

Model catalyst samples were prepared and characterized in an ultra-high vacuum (UHV) apparatus at the Charles University, equipped with x-ray photoelectron spectroscopy (XPS, hemispherical analyzer SPECS Phoibos 150 with 9-channel MCD, dual non-monochromated Al Kα/Mg Kα laboratory x-ray source SPECS XR 50), low-energy electron diffraction (LEED, SPECS ErLEED 150), a homemade scanning tunneling microscope (STM), and facilities for sample cleaning and preparation – K-type thermocouple for determining sample temperature, LN_2 sample cooling, radiation sample heating, ion gun, gas dosing system, e-beam evaporators, quartz crystal microbalance (QCM). Base pressure of the apparatus was $1 \cdot 10^{-7}$ Pa.

Nanoislands of CeO_2 were prepared by evaporating Ce metal (Goodfellow, 99.9%) from e-beam heated Ta crucible in a background pressure of $2 \cdot 10^{-5}$ Pa O_2 (5.0, Linde AG). Amount of deposited CeO_2 was determined by QCM. The mass of Ce deposited in vacuum at the sample position was measured by an Inficon 750-1000-G10 6 MHz crystal installed in a water-cooled shield and operated in the linear regime when the mass is proportional to the frequency change.[3] The thermal drift of the crystal frequency was determined separately and subtracted. Previously, this method was used in our laboratory to determine submonolayer amounts of deposited Pt.[4,5] The amount of CeO_2 was determined with an estimated error of ±10%, and expressed in terms of monolayers (ML), whereas 1 ML represents a basic O-Ce-O repeat unit of $CeO_2(111)$ containing $7.9 \cdot 10^{14}$ cm^{-2} Ce atoms, twice that O atoms, and featuring a thickness of 3.1 Å. Deposition rate was 9 ML/hour. High temperature samples (HT samples, Figure 1 a-c, Figure 2 a, c, Table S1 – samples No. 1-3) were deposited on clean Pt(111) substrates (MaTecK GmbH) at room temperature (RT), and, after deposition, annealed at 1050 K in a background pressure of $2 \cdot 10^{-5}$ Pa O_2 for 10 min. Low temperature samples (LT samples, Figure 1 d, e, Figure 2 b, d, Table S1 – samples No. 5, 6) were deposited on clean Pt(111) substrates at 523 K, and, after deposition, annealed at 850 K in a background pressure of $2 \cdot 10^{-5}$ Pa O_2 for 10 min. LT sample with 3.3 ML CeO_2 (Figure 1 e, Figure 3 b, Table S1 – sample No. 7) was prepared in two subsequent deposition and annealing steps, whereas the second step involved deposition at RT in a background pressure of $2 \cdot 10^{-5}$ Pa O_2 and subsequent annealing at 850 K in a background pressure of $2 \cdot 10^{-5}$ Pa O_2 for 10 min. Reference HT sample in Figure 3 a, Table S1 – sample 4, was prepared in two subsequent deposition and annealing steps, whereas the second step involved deposition at 1050 K in a background pressure of $2 \cdot 10^{-5}$ Pa O_2 and subsequent annealing at 850 K in a background pressure of $2 \cdot 10^{-5}$ Pa O_2 for 10 min. Reference continuous layer of $CeO_2(111)$ (Figure S4, Table S2 – sample No. 9) was prepared by deposition at 523 K in a background pressure of $2 \cdot 10^{-5}$ Pa O_2 and subsequent annealing at 523 K in a background pressure of $2 \cdot 10^{-5}$ Pa O_2 for 10 min. Other reference samples presented in SI were prepared according to the procedures for HT and LT samples.

After preparation, samples of model catalysts were characterized by STM, XPS, and LEED. STM images were obtained using chemically etched W tips at a tunneling voltage of 2 V, and tunneling currents 50-100 pA. STM images represent empty states of the samples. For each sample, several STM images were obtained at macroscopically distant positions (single millimeters) to verify a homogeneous nature of the sample morphology. Calibration of the STM magnification was performed using atomically resolved images of $CeO_2(111)$ (lateral direction), and images of monoatomic step edges of clean Pt(111) (vertical direction). STM coverage of the ceria nanoislands was determined via "Mark grains by threshold" procedure implemented in the Gwyddion software.[6] Due to tip convolution effect in STM, this procedure provides an upper estimate of the actual coverage.[7] A lower estimate of the ceria coverage was determined dividing the amount of deposited CeO_2 determined from QCM by the highest local ceria thickness (ML) identified in the STM images. A representative STM coverage θ^{Ce}_{STM} was

finally determined averaging the lower and the upper estimates for each sample (cf. Figure 4, Table S1). CeO_2 average thickness and CeO_2 maximum thickness were obtained from height distribution of the STM images obtained from the Gwyddion software. Autocorrelation length was obtained from the "2D autocorrelation" procedure implemented in the Gwyddion software. The autocorrelation length is representative of the characteristic lateral size of ceria nanoislands in all HT and LT ceria samples (Figure 1) with exception of HT ceria sample with 3.1 ML CeO_2 where the autocorrelation length is significantly reduced due to nucleation of small ceria clusters on the surface of the CeO_2(111) thin film (Figures 1 c, S2 a). Extent of the oxide/metal boundary in the samples was determined using a semi-automated procedure when first the perimeter of the ceria nanoislands in the STM images is marked manually, and the outline is projected on a properly scaled and oriented Pt(111) surface for determining the percentage of Pt surface sites occupied by the boundary (Figure S2 b).[4,5] When required for the presentation, interfering high frequency noise in the STM images was suppressed using a "Gauss filter" as implemented in the Gwyddion software, with no influence on the observable and evaluated quantities. XPS spectra of Ce 3d were fitted for Ce^{3+} and Ce^{4+} contributions using the procedure by Skála *et al*.[8] (Figure S2 c, S6).

Upon preparation and characterization in UHV, model catalyst samples were transferred to electrochemical cell for characterization by cyclic voltammetry (CV). Before the transfer, samples were shortly annealed at 850 K in a background pressure of $2 \cdot 10^{-5}$ Pa O_2 for 5 min to remove a potential damage from UHV characterization and residual adsorbates. The transfer involved 3 steps: exposure of samples to 1 atm of Ar (6.0, Linde AG) in the loadlock chamber of the UHV apparatus (~3 min.), transfer of the sample through air to the EC cell (~1 min.), and installation of the sample in Ar-filled EC cell followed by extensive Ar purging to remove the air from the cell before bringing the sample in contact with the electrolyte (~3 min.).

CV measurements were performed in a homemade glass EC cell with always freshly prepared 0.1 M KOH solution as an electrolyte. All cell parts getting into contact with the electrolyte were cleaned in a hot solution of concentrated H_2SO_4 and 30% H_2O_2, and repeatedly rinsed with hot ultrapure water (Merck Milli-Q®, 18 MΩ·cm@25°C). Electrolyte was prepared from ultrapure water, and a 30% KOH water solution (Fluka TraceSELECT®). Prior to sample transfer, the electrolyte was saturated with Ar. Measurements were performed in a hanging meniscus configuration with the sample fixed in a holder constructed from a polycrystalline Pt foil (99.95%, Safina). Reference electrode was a mercury sulfate electrode (RME 122B, Monokrystaly Turnov) connected via a salt bridge containing 0.1 M KOH solution. Electrochemical potential was recalculated to V vs. RHE using a tabulated potential of the mercury sulfate electrode 0.6513 V vs. SHE, pH=13, and T=25°C corresponding to our experimental conditions. Counter electrode was a polycrystalline Pt foil (99,95%, Safina) of ~10 cm^2 geometrical area. All measurements were performed at a scan rate of 400 mV/s to suppress the distortion of CV curves due to residual oxygen content in the electrolyte. Measurements at slower scan rates (50 mV/s) have shown the same qualitative features as presented for the measurements at 400 mV/s throughout this paper. CV curves were obtained using BioLogic SP-50 potentiostat with current-interrupt iR compensation. When required for the presentation, interfering high frequency noise in the CV curves was suppressed using a "Savitzky-Golay" smoothing as implemented in the OriginPro software,[9] with no influence on the observable and measured quantities. The electrochemically active area was considered 0.79 cm^2 (1 cm sample diameter). Faraday charges in the CV curves were integrated numerically between 0 and 0.9 V vs. RHE. Reference Faraday charges for clean Pt(111) sample (Figure S3) were determined as $q^{ref}_{H/Pt} = 350$ μC/cm^2, $q^{ref}_{DL} = 125$ μC/cm^2, and $q^{ref}_{OH/Pt} = 305$ μC/cm^2 in good agreement with values reported in the literature.[1]

After CV characterization, samples were rinsed with ultrapure water, dried with Ar, and their morphology characterized in air using AFM (Bruker MultiMode 8 AFM) in PeakForce Tapping® measurement mode. When required for the presentation, interfering high frequency noise in the AFM images was suppressed using a "Gauss filter" as implemented in the Gwyddion software, with no influence on the observable and evaluated quantities. Upon AFM characterization, samples were inserted back in the UHV chamber, evacuated and characterized with XPS.

References:

(1) Markovic, N. M.; Ross, P. N. J. Surface Science Studies of Model Fuel Cell Electrocatalysts. *Surf. Sci.Reports* **2002**, *45*, 117.

(2) Subbaraman, R.; Danilovic, N.; Lopes, P. P.; Tripkovic, D.; Strmcnik, D.; Stamenkovic, V. R.; Markovic, N. M. Origin of Anomalous Activities for Electrocatalysts in Alkaline Electrolytes. *J. Phys. Chem. C* **2012**, *116*, 22231.

(3) Sauerbrey, G. Verwendung von Schwingquarzen Zur Wägung Dünner Schichten Und Zur Mikrowägung. *Zeitschrift für Phys.* **1959**, *155*, 206.

(4) Tovt, A.; Bagolini, L.; Dvořák, F.; Tran, N.-D.; Vorokhta, M.; Beranová, K.; Johánek, V.; Farnesi Camellone, M.; Skála, T.; Matolínová, I.; *et al.* Ultimate Dispersion of Metallic and Ionic Platinum on Ceria. *J. Mater. Chem. A* **2019**, *7*, 13019.

(5) Dvořák, F.; Farnesi Camellone, M.; Tovt, A.; Tran, N.; Negreiros, F. R.; Vorokhta, M.; Skála, T.; Matolínová, I.; Mysliveček, J.; Matolín, V.; *et al.* Creating Single-Atom Pt-Ceria Catalysts by Surface Step Decoration. *Nat. Commun.* **2016**, *7*, 10801.

(6) Nečas, D.; Klapetek, P. Gwyddion: An Open-Source Software for SPM Data Analysis. *Open Phys.* **2012**, *10*, 181.

(7) Lykhach, Y.; Kozlov, S. M.; Skála, T.; Tovt, A.; Stetsovych, V.; Tsud, N.; Dvořák, F.; Johánek, V.; Neitzel, A.; Mysliveček, J.; *et al.* Counting Electrons on Supported Nanoparticles. *Nat. Mater.* **2016**, *15*, 284.

(8) Skála, T.; Šutara, F.; Prince, K. C.; Matolín, V. Cerium Oxide Stoichiometry Alteration via Sn Deposition: Influence of Temperature. *J. Electron Spectros. Relat. Phenomena* **2009**, *169*, 20.

(9) OriginPro, Version 2020b. OriginLab Corporation, Northampton, MA, USA.